A Convolutional Neural Network to Locate Unbalance in Turbomachinery Supported by AMBs

Giovanni Donati
Department of Information Engineering
University of Florence
Florence, Italy
giovanni.donati@unifi.it

Michele Basso
Department of Information Engineering
University of Florence
Florence, Italy
michele.basso@unifi.it

Marco Mugnaini
Department of Information Engineering and Mathematics
University of Siena
Siena, Italy
marco.mugnaini@unisi.it

Chiara Camerota
Department of Information Engineering
University of Florence
Florence, Italy
chiara.camerota@unifi.it

***Abstract*— Due to the complex structure of turbomachinery systems, the process of fault detection assumes paramount importance, in particular rotor unbalance faults are particularly risky and common. This research paper introduces an innovative and straightforward approach to locate rotor unbalance faults for turbomachinery supported by Active magnetic bearings (AMB) exploiting the AMB sensors and utilizing Deep Learning techniques (1D Convolutional Neural Networks). The main goal of this study is to develop a fault dictionary, built using fault signatures derived from position sensor signals, and a classifier specialized in locating the unbalance faults in turbomachinery supported by AMBs, that generally occur in the turbomachine impellers. These are the most prevalent unbalance faults that affect turbomachinery systems and that commonly impact the performance of AMB systems. The effectiveness of this approach is demonstrated through a case study involving an expander-compressor supported by two active magnetic bearings in the oil and gas field. Five distinct fault classes are considered, and the neural network fault classifier achieves an impressive accuracy rate of 98% on the test dataset.**

Keywords—Active Magnetic Bearings, AMB, Rotor fault, Unbalance Fault, Convolutional Neural Networks

I. INTRODUCTION

Active Magnetic Bearings (AMBs) are becoming increasingly important in a wide range of rotating machinery applications. These applications can vary from small turbo molecular pumps used in medicine to large megawatt-scale compressors used in the oil and gas industry. Unlike traditional contact bearings, AMBs offer significant advantages. One key benefit is their ability to eliminate friction and wear by levitating the rotor with respect to the stator components. This enables higher rotational speeds, improves system efficiency, and eliminates the need for complex lubrication systems typically found in traditional bearings. However, due to their inherently unstable nature, AMBs require a feedback control system to operate. This closed loop comprises different components, including controller, position sensors, amplifiers and actuators. A detailed description of the structure of AMB systems can be find in [1]. The AMB system component choice determines the nominal stiffness and damping characteristics of the bearings. These properties establish the overall stability and performance of the closed-loop system. Beyond the already mentioned advantages, AMBs can be exploited for fault location and even for fault compensation. In fact, the sensors on board AMB systems allow for continuously monitoring the behavior of the rotor during operations and provide information useful for detecting faults, ensuring safe and reliable operation.

The early detection of failures in AMB systems offers the opportunity to employ safety strategies that leverage the closed-loop architecture to adapt the system and respond to the detected faults in real-time. The active nature of AMB controllers allows for dynamic adjustments to the bearing behavior, enhancing the system chances of survival exploiting an internal information processing. Consequently, fault tolerant AMB systems have been developed to effectively manage malfunctions, utilizing for example reconfigurable control strategies [2]. As a result, numerous research studies have focused on developing methods to identify failures associated with the rotor or the electrical and electronic components.

A common practice to identify faults involves the use of system observers that compare the system state with the expected one related to the normal operational condition to identify any anomalies. A different approach is the simulation-before-test technique. This method involves creating a fault dictionary through simulations of a specific system [3], which accumulates instances of fault signatures, and these signatures serve as training data for a classifier capable of recognizing various faults, as elucidated in reference [4]. Traditionally, fault diagnosis has revolved around analyzing signals in the time and frequency domains. A similar methodology is put forth by Jing *et al.* in [5], who proposed a feature-based learning and fault diagnosis method for gearbox condition monitoring.

However, some advanced techniques exploit a fault dictionary composed of images generated from time-domain signals. These representations serve as the base for training convolutional neural networks (CNNs) specifically designed for the purpose of detecting and recognizing faulty conditions. This method applied to AMB systems was pioneered by Yan *et al.*, who employed sensor signals to construct orbits for detecting mechanical failures, as outlined in reference [6].

This research focuses on detecting and locating unbalance faults in the impellers of a turbomachine supported by AMBs in operating condition, that is one of the most common situations that occurs in a turbomachine [7] using AMBs as an identification and diagnosis tool for the system. In the context of this work, only single unbalance faults have been considered for simplicity, but the fault classes can be extended. The proposed work introduces a novel approach which aims at locating impeller unbalance faults through the application of CNN by dividing the impeller into different circular sectors and assigning to each region a different class label. The approach is demonstrated in a specific case in this paper but is a general procedure which allows for enhancing the accuracy of unbalance location by increasing the number of circular sectors. This work should be considered as an extension of the authors' work [4] which had the objective of identifying electrical faults in AMB systems. The new approach can be used together with the one previously developed.

To construct the fault dictionary, the position sensor electrical signals are harnessed as sources to generate generalized orbits, which are then transformed into discrete black and white images. The properly trained CNN, known for its proficiency

in image classification has the dual objective of identifying the defective impeller and precisely determining the location of the unbalance fault within said impeller. More specifically, the approach followed employed 1D CNNs, which exhibit great performance, as evidenced in [8], working with grid-like topological data. Furthermore, by employing computationally efficient image processing techniques, that is Adam optimization [9], in conjunction with efficient neural networks, it becomes feasible to construct an automatic online diagnostic system with minimal computational overhead.
The paper structure is the following: Section II describes the fault dictionary building process. Section III describes the proposed model of classifier trained with the fault dictionary described in the previous section. Section IV presents a case study and the obtained results. Conclusion follows.

II. Fault Dictionary Building

A. System Modeling

An AMB consists of a pair of opposing electromagnets, which exert attractive forces on a ferromagnetic object, in this case, the rotor. Their objective is to maintain the rotor in the center of the air gap. Typically, a turbomachine is equipped with no fewer than five AMBs, consisting of four dedicated to managing the radial dynamics of the rotor (two for each radial bearing) and one dedicated to controlling the axial dynamics. This study focuses exclusively on the radial dynamics of the system since radial rotor dynamics tend to be inherently more complex than its axial counterpart.

Since AMBs are inherently unstable components, they are always inserted into a stabilizing closed-loop system. Fig. 1 presents a block diagram illustrating the closed-loop configuration of an AMB system. This system includes amplifiers that drive in current the magnetic bearings, position sensors accompanied by their associated conditioning electronics, as well as a controller.

The role of the position sensors is to continuously monitor the rotor position, providing real-time data. The controller leverages these position signals to compute the required control inputs for the actuators, which drive the magnetic bearings. The main objective of this closed-loop system is to consistently maintain the rotor in a suspended state at the center of the air gap. This is achieved by determining the optimal control currents to drive each individual AMB.

To model the closed-loop AMB system, a state-space formulation was developed for each component. The rotor radial state-space model was specifically constructed using a finite element method (FEM) using Timoshenko modeling [10]. Additionally, linear state-space models were used to describe the electrical components of the AMB system, considering their unique characteristics and specifications. Combining the rotor state space and the electrical component models, a closed-loop system state space was found:

$$\frac{d}{dt}\begin{bmatrix}X_R\\X_B\end{bmatrix} = \begin{bmatrix}A_R & B_R C_B\\ B_B C_R & A_B\end{bmatrix}\begin{bmatrix}X_R\\X_B\end{bmatrix} + \begin{bmatrix}B_R\\[0]\end{bmatrix} F_{ext} =$$

$$= A\begin{bmatrix}X_R\\X_B\end{bmatrix} + BF_{ext} \quad (1)$$

where X_R and (A_R, B_R, C_R) represent the state and the matrices of the rotor model, X_B and (A_B, B_B, C_B) are the state and matrices of the second state space of the electrical models and F_{ext} the external forces acting on the system. Equation (1) allows for studying the performance and dynamic behavior of the AMB system model.

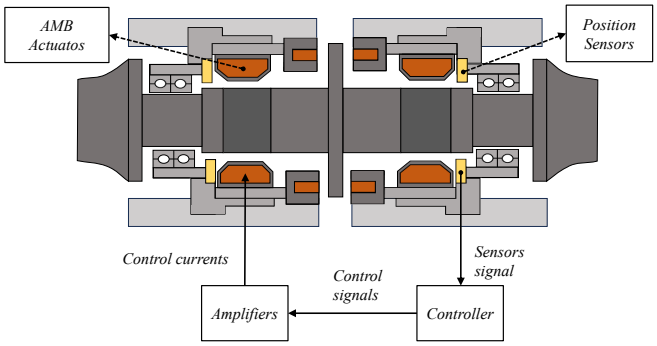

Fig. 1. Schematic of an AMB system structure.

In high-speed turbomachine, the main contribution of the term F_{ext} is the unbalance force. Unbalance forces are synchronous with the rotor speed and arise from the existence of unbalanced masses relative to the rotor axis of rotation. These unbalanced masses result from inherent manufacturing imperfections or arise from wear. When considering a fixed rotor speed Ω along a given axis x, an unbalance force is added to F_{ext}, which takes the following expression:

$$F_{un_x} = \Omega^2 U\cos(\Omega t + \phi) \quad (2)$$

where ϕ is the phase of the unbalance with respect to other axis and U is the unbalance magnitude in kgm. To exactly reproduce the dynamic behavior of a real system, each machine is experimental identified to accurately assess the unbalance and to fine tune the state-space model (1), as for example accurately described in [11].

B. Unbalance Fault

Due to the complex mechatronics nature of AMB systems, failures can manifest in different ways, software, electrical, or mechanical, which can impact system performance differently. Lijesh *et al.* in [12] summarizes common malfunction causes, their occurrence, and severity. These faults can lead to high-speed rotor contact with the housing, exposing plant safety. To mitigate these risks, measures like redundancies, quality control, individual actions, and various control strategies are essential. Active fault diagnostics and corrections are also valuable. This work focuses on unbalance faults, whose action on the AMB closed-loop system can be modeled by (2). Even if the rotor is balanced in the manufacturing process, a residual unbalance always remains. Following an identification process this unbalance is measured and characterizes the particular turbomachine. During normal operation, thanks to AMB levitation, wear mainly occurs only on the impeller blades. Solid particle erosion is one of the main reasons causing the blades wear failure. Wang *et al.* in [13] analyzed the primary influencing factors on erosion such as the particle characteristics, environmental condition, and materials characteristics. Normally, the worn blades must be localized and repaired in an impeller. Every worn blade act as an unbalance fault that contributes to the vibrations of all the AMB closed-loop system.

This work aim is to localize the faulty impeller and the position of the faulty blade, considering a single fault at a time. More specifically, the localization is intended as the identification of the phase ϕ between the native unbalance ($\phi = 0^o$) of the particular turbomachine and the faulty blade. To this aim, the impeller is divided into equal circular sectors and the aim of this work is to locate the sector that contains the faulty blade. Fig. 2 summarizes this idea. In this work, for demonstration purposes, only two circular sectors (β_1 and β_2) per impeller were considered but the sector number can be arbitrarily increased if needed.

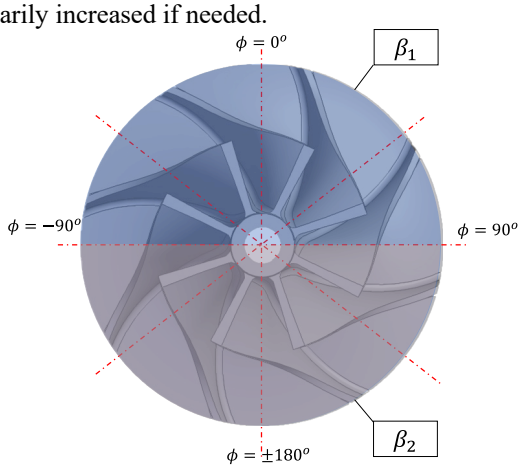

Fig. 2. Impeller sector division.

C. Fault Dictionary

Steady-state signals are exploited to construct images that serve as fault signatures, which act as input data to train a classifier. In this work, position signals from sensors that are always available in an AMB system are considered.
Considering that all signals inherently present periodic behavior when the turbomachine operates at a fixed rotational speed, under steady conditions, it becomes feasible to organize these time signals into couples, by expressing the signal associated with one of the two orthogonal control axes of a radial AMB as a function of the other. In this process, time is no longer treated as an independent variable, and one generalized signal trajectory or orbit is generated for each radial bearing. In the presence of a fault these orbits change assuming specific and peculiar shapes corresponding to the related fault. Therefore, the collection of the different orbit signatures in the presence of different faults can be used as a fault dictionary.

The fault orbits were derived through the utilization of a simulation tool capable of automatically building the entire fault dictionary modeling the fault conditions, as described in [3]. This simulation tool has been implemented within the Matlab-Simulink environment and enables the accomplishment of Monte Carlo simulations by using specific probability distributions to simulate the parameter variation ranges of the AMB system components or by adding noisy signals. The developed simulation tool was validated by comparing the results obtained with commercial software (MADYN 2000). To create reference orbits linked to the non-faulty condition, machine operations at a constant rotor speed were simulated while varying the component parameters within their specified tolerance ranges and accounting for normal level of noise. The dictionary is completed by collecting the orbit orbits linked to faulty conditions obtained simulating the different impellers unbalance faults by randomly varying different unbalance phases and magnitudes. Variations within component parameter tolerance ranges define confidence regions containing the reference orbits representing the fault-free condition. Any deviations of the orbits outside these regions signify a fault occurrence. The orbit signatures were represented by images with a fixed resolution. Black and white images were generated through the Matplotlib library in Python. Utilizing images directly from the available signals to train a classifier enhances the system capability to comprehend the AMB system state. This approach provides a broader perspective and improves the precision of captured information.

III. Convolutional Neural Networks

The unbalance fault localization issue can be considered as a classification problem. A CNN-based classifier was developed to address the sensor orbit images. This model is tailored to handle grid-like topological data, encompassing a wide range of data types that can be conceptualized as either 1D or 2D grids, including time-series data and images. AlexNet, introduced by Krizhevsky *et al.* in [14], emerged as the pioneer of modern deep CNNs in the realm of image classification. The CNN architecture comprises sequential layers, organized as follows: convolutional layers, triggered by a chosen activation function, pooling layers, and fully connected layers. A convolutional layer involves sliding a filter/kernel across the input data, performing convolutions. Depending on patterns and spatial information, a filter can extract various features, yielding a feature map as its output. The activation function serves to introduce non-linearity into the network, with ReLU and its derivatives being the most prevalent choices [15]. The pooling layer plays a dual role in neural networks; it extracts essential information from the feature map while concomitantly diminishing computational complexity. For instance, a widely employed technique is Max pooling [16], wherein the highest value within a given region signifies the entire content of that region. Finally, the feature map is flattened into a one-dimensional array and fed into the fully connected layers for classification and prediction. The choice of the final function depends on the particular task. For multivariate classification problems, one common choice is the SoftMax function [17]. To evaluate the error, i.e., the disparity between the prediction and the actual value, a loss function is employed. Once again, the choice of this function is contingent on the nature of the problem being addressed. An optimization algorithm is then utilized to minimize the loss function and refine the accuracy of the network predictions. A frequently used algorithm is the Adam Optimizer and its variants [9]. In summary, the input data undergoes a series of transformations through the convolutional layer, followed by summarization, flattening, and prediction computation. This iterative process involves updating the network weights to minimize the loss function, enhancing the accuracy of predictions with each iteration.

IV. Case Study and Results

A. Case Study Description

As a case study to assess the performance of the proposed diagnosis method a medium size expander-compressor

supported by AMBs for oil and gas application was considered. The rotor has a mass of about 220 kg and a length of about 1.233 m. For what concerns the electrical part, the controller structure was composed by augmented PIDs. Additionally, other components included switching pulse width modulation (PWM) amplifiers coupled with heteropolar AMB actuators and inductive position sensors operating within a 2.5 kHz bandwidth. Under nominal conditions, the system features a nominal rotation speed of 6920 rpm and a native unbalance of 1.45×10^{-4} kgm positioned at the center of mass of the rotor.

For this case study, tolerance parameters encompassed a 2% variation in sensor sensitivities, sensor biases of 1 μm, and Gaussian white noise characterized by a standard deviation of 1 μm. Regarding the actuators, a 2% tolerance of the DC gain was taken into consideration. Since the number of impellers of the system is two, the fault classes considered were four, considering two circular sector per impeller (β_1 and β_2), as shown in Fig. 2. The five classes and the number of examples per class are summarized in Table I. The faulty conditions that were taken into account to form the classes of the fault dictionary were simulated with a Monte Carlo analysis by varying the fault unbalance magnitude in the range $[0, 6.00 \times 10^{-4}]$ kgm and its phase in the prescribed range using a uniform distribution.

TABLE I.

Class Name	*Example Class Size*
Nominal Condition	3000
Expander fault in β_1	2000
Expander fault in β_2	2000
Compressor fault in β_1	2000
Compressor fault in β_2	2000

B. *Proposed CNN Model*

As anticipated, the CNN classifier is designed with the specific aim of identifying five classes: the Nominal Condition, two unbalance faults on the expander impeller and two unbalance faults on the compressor impeller. The classifier structure is illustrated in Fig. 3. It comprises a series of stacked convolutional, pooling, and fully connected layers. The input to the network consists of a grayscale image depicting two orbits from sensors, one for each AMB, while the output gives the probability distribution across the five classes. As previously mentioned, when the activation function triggers a convolutional layer, it extracts key features utilizing filters. These outputs are then aggregated through max-pooling and subsequently classified by the fully connected layers. All convolutional layers employed are 1D, simplifying network complexity and computational load. They have a kernel dimension of 3×3, and a stride dimension of 1×1, activated by a ReLu function [15]. The max-pooling operation is executed with a stride dimension of 2×2. The initial convolutional layer features one input channel and produces eight output channels. The second convolutional layer mirrors this configuration with eight input and output channels. This approach is employed to expand and then consolidate information, emphasizing critical features. This process also serves to mitigate gradient explosion following a max-pooling layer. Subsequently, a batch normalization step is implemented to preclude dropout usage, as demonstrated in [18]. This ensures that initialization does not unduly impact results. The final two convolutional and max-pooling layers are helpful in amalgamating and distilling output from preceding layers, extracting only the most significant features, including intricate patterns and structures. Subsequently, the fully connected component commences. Initially, the data vector undergoes a transformation into a one-dimensional tensor, after which three linear layers are trained. These layers progressively reduce the vector dimension until arriving at the five classification classes. In this study, an Adam Optimizer [9] was employed to optimize algorithm efficiency, balancing computational resources and memory usage. The architectural implementation was executed utilizing the PyTorch libraries.

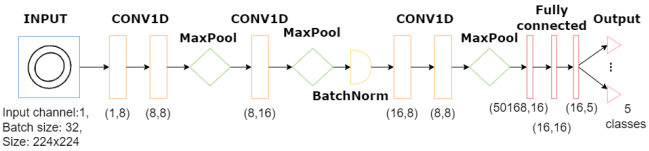

Fig. 3. CNN proposed model structure, the numbers below the layer represent the input and output channels.

C. *Results*

The dataset, obtained as described in the previous section, is composed of 3000 examples of the fault free condition and 2000 examples for each of the other 4 fault classes. The training set includes 80% of the examples and the test and a validation set collects 10 % of the remaining examples each. Each image had a size of 224×224 pixel.

The model was trained using the pre-processed training set (employing a batch size of 32) for a total of 300 epochs, using a learning rate of 10^{-6}. This training process took approximately 4 hours, utilizing a GPU NVIDIA RTX A6000 with 48 GB GDDR6. Validation of the proposed Convolutional Neural Network (CNN) was carried out using the test dataset, where it achieved an accuracy of approximately 98%. Simultaneously, the training dataset yielded an accuracy of around 99%. The obtained interference time is 2×10^{-4} s, thereby validating the feasibility of implementing the proposed model in real-time applications. These results are graphically represented in Fig. 4 and Fig. 5 showcasing respectively test set accuracy and training set performance.

Fig. 6 illustrates the test and accuracy ratio, which shows the relationship between the training and test accuracies depicted in Fig. 4 and Fig. 5. The declining trend observed in this graph suggests that the estimated parameters of the CNN remain unaffected by overfitting. This observation implies that the model has achieved a good level of generalization, indicating its capability to effectively apply learned patterns and make accurate predictions when confronted with previously unseen data.

Furthermore, Fig. 7 presents the resulting confusion matrix, in which the horizontal axis represents the actual faults, and the vertical axis represents the predicted faults. The diagonal elements represent the percentage of accurate predictions, while values above the diagonal denote false positives, and those below signify false negatives. As depicted in Fig. 7, the confusion matrix displays a notably

diagonal pattern, with even the lowest values hovering around 98%. Most misclassifications primarily are associated with minor parametric deviations from the fault-free condition. The achieved accuracy in recognizing these faults, even with small parametric variations, is quite satisfactory for two key reasons. First, the regions of parameter variation related to faults closely border the tolerance regions. Second, the limited image resolution contributes to some classes being recognized less accurately, specifically those associated with orbits that exhibit minor differences compared to the reference orbits when subjected to slight parameter variations beyond the tolerance, as there are no clear-cut boundaries between faulty and fault-free conditions. However, it's worth noting that false positives or negatives in these borderline situations do not have significant consequences.

Similar accuracy was also achieved in [4] where a 3D convolutional neural network was implemented to identify electrical faults, and in [19] where several convolutional neural networks were tested to identify simpler mechanical faults.

IMG

Fig. 4. Train accuracy for each epoch.

IMG

Fig. 5. Test accuracy for each epoch.

IMG

Fig. 6. Train and test accuracy ratio plot.

V. Conclusion

Active Magnetic Bearings are gaining prominence across various rotating machinery applications owing to their exceptional performance and the elimination of cumbersome lubrication systems. However, their operation necessitates a complex closed-loop mechatronic system. To ensure safe and reliable operation, the deployment of fault detection and diagnostic systems becomes imperative.

The novel approach presented here for fault diagnosis leverages sensor signals within an AMB system to build a fault dictionary with the aim of training a classifier – a straightforward convolutional neural network. This classifier has been specifically trained to locate the unbalanced faults in the turbomachine impellers. The proposed classifier demonstrates remarkable accuracy and generalizability, all while requiring a modest amount of data. Importantly, this approach can be readily extended to address other fault types and can be applied to a variety of AMB-supported systems systems.

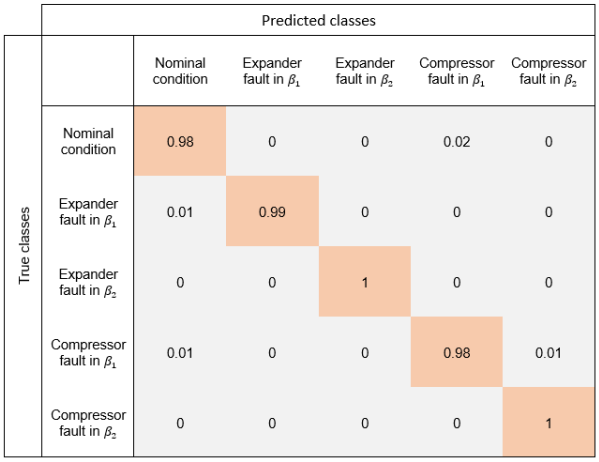

Fig. 7. Confusion matrix of test set.

References

[1] Srinivas R. S., Tiwari R., Kannababu C, "Application of active magnetic bearings in flexible rotordynamic systems–A state-of-the-art review," Mechanical Systems and Signal Processing, vol. 106, pp. 537-572, 2018.

[2] Tsai N. C., King Y. H., Lee R. M, "Fault diagnosis for magnetic bearing systems. Mechanical systems and signal Processing," vol. 23(4), pp. 1339-1351, 2009.

[3] M. Basso, G. Donati and M. Mugnaini, "Smart Fault Dictionary for Active Magnetic Bearings Systems," 2023 IEEE International Workshop on Metrology for Industry 4.0 & IoT (MetroInd4.0&IoT), Brescia, Italy, 2023, pp. 360-365, doi: 10.1109/MetroInd4.0IoT57462.2023.10180183.

[4] Donati G., Basso M., Manduzio G. A., Mugnaini M., Pecorella T., Camerota C., "A Convolutional Neural Network for Electrical Fault Recognition in Active Magnetic Bearing Systems," Sensors, vol- 23, no. 16, 7023, 2023.

[5] Jing L., Zhao M., Li P., Xu X. A convolutional neural network-based feature learning and fault diagnosis method for the condition monitoring of gearbox. Measurement, , vol. 111, pp. 1–10, 2017

[6] Yan X., Zhang C. A., Liu Y., "Multi-branch convolutional neural network with generalized shaft orbit for fault diagnosis of active magnetic bearing-rotor system," Measurement, vol. 171, 108778, 2021.

[7] Zabihihesari A., A. Shirazi, F., Riasi A., Mahjoob M., Asnaashari E., "Simulation-based Vibration Sensor Placement for Centrifugal Pump Impeller Fault Detection," Journal of Computational Applied Mechanics, vol. 51, no. 1, pp. 72-80, 2020.

[8] Junior R. F. R., Dos Santos Areias I. A., Campos M. M., Teixeira C. E. da Silva L. E. B., Gomes G. F., "Fault detection and diagnosis in electric motors using 1d convolutional neural networks with multi-channel vibration signals," Measurement, vol. 190, 110759, 2022.

[9] Kingma D. P., Ba J., "Adam: A Method for Stochastic Optimization*," ArXiv. /abs/1412.698*, 2014.

[10] Friswell M. I., Penny J. E., Garvey S. D., Lees A. W., Dynamics of rotating machines. Cambridge university press, 2010.

[11] Wroblewski A. C., Sawicki J. T., Pesch, A. H., "Rotor model updating and validation for an active magnetic bearing based high-speed machining spindle," Journal of Engineering for Gas Turbines and Power, vol. 134, no. 12, 122509, 2022.

[12] Lijesh K. P., Hirani H, "Failure Mode and Effect Analysis of Active Magnetic Bearings," Tribology in Industry, vol. 38.1, 2016.

[13] Wang G., Jia X., Li J., Li F., Liu Z., Gong B., "Current state and development of the research on solid particle erosion and repair of turbomachine blades," In Re-engineering Manufacturing for Sustainability: Proceedings of the 20th CIRP International Conference on Life Cycle Engineering, Singapore 17-19 April, pp. 633-638, 2013.

[14] Krizhevsky Alex, Ilya Sutskever, Geoffrey E. Hinton, "Imagenet classification with deep convolutional neural networks," *Communications of the ACM,* vol. 60, no. 6, 2017, pp. 84-90.

[15] Agarap A. F., "Deep learning using rectified linear units (relu)," arXiv preprint arXiv:1803.08375, 2018.

[16] J. Nagi et al., "Max-pooling convolutional neural networks for vision-based hand gesture recognition," 2011 IEEE International Conference on Signal and Image Processing Applications (ICSIPA), Kuala Lumpur, Malaysia, 2011, pp. 342-347, doi: 10.1109/ICSIPA.2011.6144164.

[17] Liu W., Wen Y., Yu Z., Yang M., “Large margin softmax loss for convolutional neural networks,” arXiv preprint arXiv, 1612.02295, 2016.

[18] Ioffe S., Szegedy C., “Batch Normalization: Accelerating Deep Network Training by Reducing Internal Covariate Shift,” *ArXiv. /abs/1502.0.*

[19] Y. Hu, O. W. Taha, K. Yang, "Fault Detection in Active Magnetic Bearings Using Digital Twin Technology" Applied Sciences, Vol. 14, no. 4: 1384, 2024. doi: 10.3390/app1404138